Zeitschrift: Helvetica Physica Acta

Band: 58 (1985)

Heft: 2-3

Artikel: Electro-optical light modulation in a GaAs/AlGaAs multiquantum well heterostructure

Autor: Glick, M. / Reinhart, F.K. / Weimann, G.

DOI: https://doi.org/10.5169/seals-115608

Helvetica Physica Acta, Vol. 58 (1985) 403–409

0018–0238/85/020403–07$1.50 + 0.20/0

Electro-optical light modulation in a GaAs/AlGaAs multiquantum well heterostructure

By M. Glick and F. K. Reinhart

Institut de physique appliquée, Ecole Polytechnique Fédérale de Lausanne, PH-Ecublens, CH-1015 Lausanne

and

G. Weimann

Forschungsinstitut der DBP, D-6100 Darmstadt

(1. XI. 1984)

In honor of Emanuel Mooser's 60th birthday

Abstract. The linear electro-optic coefficient r_{41} has been determined in a GaAs–AlGaAs multiquantum well waveguide structure consisting of 30 GaAs quantum wells 122 Å thick and 29 AlGaAs barriers 182 Å thick. The value was found to be $r_{41} = -1.47 \times 10^{-10}$ cm/V at $\lambda = 1.1523$ μm.

We have determined the linear electro-optic (LEO or Pockel's) effect in a GaAs-AlGaAs multiquantum well (MQW) heterostructure p-n junction diode at $\lambda = 1.1523$ μm. MQW structures have been shown to have valuable properties as diode lasers [1] and modulators [2]. Little information is available as to their properties as optical waveguides. In particular we can examine how these properties become manifest in optical modulators. For this, we chose to use a wavelength far from the observed room temperature excitonic peak of 0.858 μm in order to obtain results where the LEO effect is dominant.

The MQW structure properties should vary from those of a random alloy $Al_xGa_{1-x}As$ having a corresponding Al content [3, 4]. Because of the layered nature of the MQW film we also expect a relatively large birefringence [5]. It is of interest to determine if this layering adds any unforeseen morphological effects [6] that modify the LEO effect.

For our experiment, the MQW waveguide structure was fabricated by molecular beam epitaxy on a Si-doped n^+ type GaAs substrate ($n^+ \approx 10^{18}$ cm^{-3}) oriented on a crystallographic (001) plane. A Si-doped n^+ GaAs buffer layer ($n^+ \approx 10^{18}$ cm^{-3}) was grown first, followed by a Si-doped $Al_{0.24}Ga_{0.76}As$ cladding layer about 1.84 μm thick. Its doping was nominally $n = 3.4 \times 10^{17}$ cm^{-3}. This was followed by 30 undoped 122 Å thick GaAs quantum well layers separated by 182 Å thick undoped $Al_{0.24}Ga_{0.76}As$ barrier layers, a Be-doped ($P = 3 \times 10^{17}$ cm^{-3}) cladding layer of 1.96 μm thickness and a Be-doped contact layer with doping in the 10^{19} cm^{-3} range. A schematic of the sample is shown in Fig. 1.

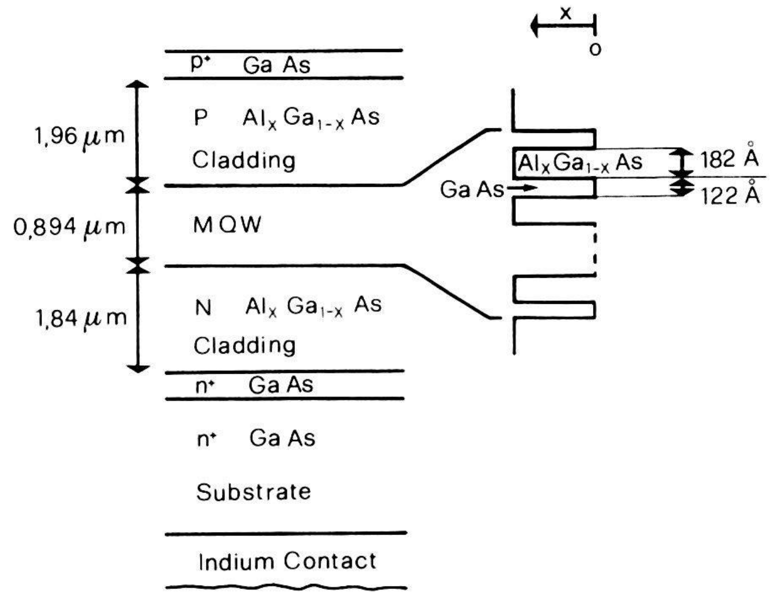

Figure 1
Schematic of the MQW structure. The insert schematically shows the Al concentration x to vary from $x = 0$ to $x = 0.24$.

Room and low temperature luminescence measurements were used to verify the aluminium content of 24%.

A $1.09 \times 0.9\ \mathrm{mm}^2$ sample was cleaved to allow measurements of the phase modulation along the orthogonal crystallographic [110] and [$\bar{1}$10] directions. Electrical contacts were provided with indium to the substrate and to the p^+-GaAs. The sample was placed in a gold plated holder for electrical and optical measurements. Despite the fairly crude nature of the contacts, current voltage measurements show a relatively good characteristic as given by Fig. 2. The break in the reverse part of the characteristic indicates some leakage mechanisms. The

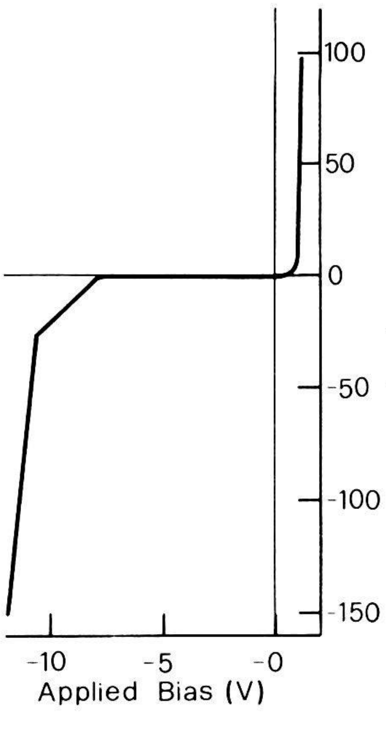

Figure 2
Current-voltage characteristic of the MQW device.

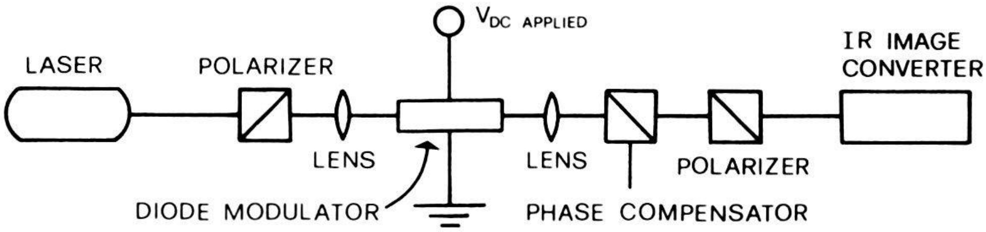

Figure 3
Experimental arrangement used for the measurement of the phase modulation.

reverse breakdown voltage, $V_B \approx -11$ V, and the series resistance, $R_s < 400\ \Omega$, were sufficient to permit strict DC measurements from +1.0 V to −10.0 V. The contacts are not sufficient for high quality capacitance measurements, capacitance versus voltage measurements taken at 100 Hz and 200 Hz yielded an approximate value of $6 \times 10^{15}\ \mathrm{cm}^{-3}$ for the effective doping of the MQW layer. With this doping level a reverse bias, $V_a = -2$ V, suffices to completely sweep out the MQW region.

For the optical measurements we used an apparatus as schematically shown in Fig. 3. A helium neon laser operating at $\lambda = 1.1523\ \mu$m was the source. Both TE and TM modes were excited by a focussed beam with polarization oriented at 45° to the junction electric field which is parallel to the crystallographic [001] direction. Phase difference measurements were made by inserting a ZEISS magnesium fluoride compensator in phase substraction position ahead of the crossed analyzer Glan–Thompson prism. The transmitted intensity minima were detected by observing the near field pattern of the exit face in the image converter.

We found it necessary to provide the four mirror faces with anti-reflection coatings in order to suppress Fabry–Perot resonances. This was achieved by anodizing the sample in $H_2O + H_3PO_4$ at pH = 2.5. To protect the electrical contact during the process the indium under the substrate and the face opposite were both masked with black wax. Not knowing the precise index of refraction of the oxide, n_{0x}, we chose a voltage of 82 V in order to obtain a coating thickness in the vicinity of $\lambda/4n_{0x}$. Compared to an uncoated GaAs surface, we measured a reflectivity of 0.9% for a planar light beam of $\lambda = 1.1523\ \mu$m.

The measured phase differences are reduced per unit length and are shown in Fig. 4. We can see that the results are clearly dominated by the LEO effect. The intersection point gives the result in phase difference, $\Delta\phi_0 = 1790$ nm/mm, which corresponds to 560 degree/mm.

GaAs and AlGaAs are both of the $\bar{4}3$ m point group. Accordingly, if only a LEO effect were involved the phase differences should change only in sign when the wave propagation direction is changed from the crystallographic [110] to the [$\bar{1}$10] direction [6]. The phase differences yield the slopes −8.31 degree/V mm and 7.70 degree/V mm for the [110] and [$\bar{1}$10] directions respectively. The discrepancy will be discussed below.

To understand the general features of these results we start from an extended MQW layer structure upon which a uniform field is applied normal to the [001] layer plane. To simplify matters further we are assuming no morphic effects due to the layering structure. This is to say we retain the $\bar{4}3$ m symmetry. However, we know that the layering induces a birefringence whose extraordinary index of refraction is perpendicular to the layer plane.

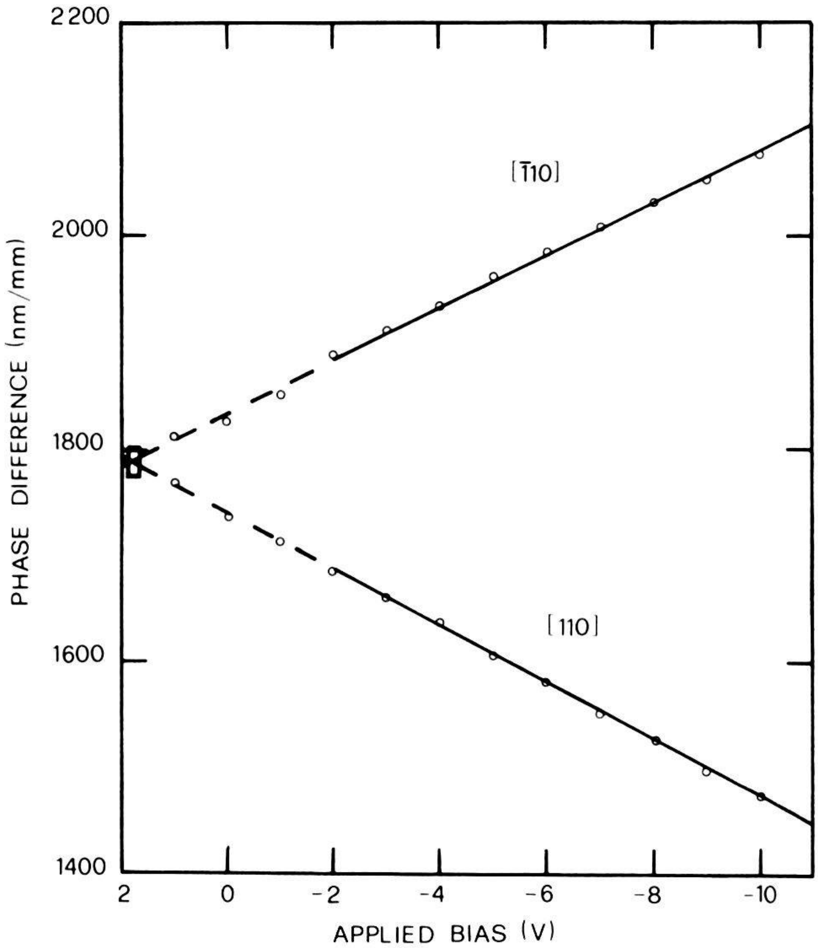

Figure 4
Phase difference between TE and TM modes as a function of the aplied bias for the two orthogonal light propagation directions along [110] and [$\bar{1}$10]. The solid lines are linear fits to the data for $V_a < -2$ V. Their extensions for $V_a > 2$ V are dashed.

By examining the boundary value problem for plane waves we obtain for the mean refractive indices of the layers, $n_\parallel$ and $n_\perp$, which relate to the polarization of the optical electric field vector parallel or perpendicular to the MQW film layer [5].

$$n_\parallel^2 = \frac{d_1 n_1^2 + d_2 n_2^2}{d_1 + d_2}$$

$$n_\perp^2 = \frac{n_1^2 n_2^2 (d_1 + d_2)}{d_1 n_2^2 + d_2 n_1^2}$$

The optical dielectric constants $n_1^2 = 11.868$ and $n_2^2 = 11.053$ and their corresponding layer thicknesses d_1 and d_2 refer to the alternating GaAs and AlGaAs layers respectively [7, 8]. For our structure with a finite layer number, we replace d_1 by $30d_1$ and d_2 by $29d_2$ to obtain $n_\parallel^2 = 11.387$ and $n_\perp^2 = 11.373$.

The birefringence of the stress free MQW structure is modified by the applied electric field according to the LEO coefficient r_{41}. Diagonalizing the relative dielectric impermeability tensor results in three indices of refraction, $n_\perp$ which is parallel to the [001] direction, and

$$n_{[110]} = n_\parallel(1 + n_\parallel^2 r_{41} E_j/2) \quad \text{and} \quad n_{[\bar{1}10]} = n_\parallel(1 - n_\parallel^2 r_{41} E_j/2)$$

for light propagating in the crystallographic [110] and [$\bar{1}$10] directions respectively. We take E_j to be the average junction electric field.

For our waveguiding problem we take the MQW layer sandwiched between the isotropic AlGaAs cladding layers. For the wavelength considered our structure permits the propagation of only the lowest order TE and TM modes whose propagation constants are described by β_{TE} and β_{TM} respectively. The total phase difference then becomes

$$\Delta\phi = (\beta_{TE} - \beta_{TM})l$$

where l is the diode length.

The contribution to the phase difference due to the electro-optic effect can be expressed as

$$\Delta\phi_{EO} = \pm\pi\Gamma n_{\parallel}^3 r_{41} E_j l/\lambda$$

The positive and negative signs are to be taken for the propagation along the crystallographic [110] and [$\bar{1}$10] directions respectively.

The factor Γ accounts for the overlap of the junction electric field with the optical field distribution [9]. For the lowest order modes the optical field distribution is proportional to a cosine function in the MQW region. The junction electric field, however, varies linearly. Once the entire MQW region is swept out, increasing the applied reverse bias yields a trapezoidal junction electric field distribution that leaves the overlap factor unchanged. The average junction electric field is obtained by $(V_0 - V_a)/d_{MQW}$, where V_0 is the built-in potential and $d_{MQW} = 30d_1 + 29d_2$ the width of the MQW. Using the average junction electric field, Γ assumes the value of 0.81 for the data given above.

The measurements yield $r_{41} = -1.53 \times 10^{-10}$ cm/V and $r_{41} = -1.42 \times 10^{-10}$ cm/V with the light propagation along the [110] and [$\bar{1}$10] directions respectively. The r_{41} values are not equal within the 1.7% error limit. Taking the average of the r_{41} values we obtain $r_{41} = [-1.47 \pm 0.03] \times 10^{-10}$ cm/V. It is of interest to note, however, that the estimated r_{41} value of the comparable homogeneous layer, $Al_{0.14}Ga_{0.86}As$, is $r_{41} = -1.43 = 10^{-10}$ cm/V, lower than our experimental value for the MQW. The value found here is closer to that of pure GaAs, $r_{41} = -1.50 \times 10^{-10}$ cm/V.[10]

The discrepancy in the results for the two directions can arise from quadratic electro-optic effects, as has been shown for InGaAsP/InP double heterostructure diodes [11], or it can also be a morphic effect due to the MQW layers. We can make an estimation of the size of a possible quadratic effect by examining the deviation of our experimental data from the average linear effect. The deviation of 3.7% at $V_a = -10$ V gives $R_{11} - R_{12} = -5.2 \times 10^{-17}$ cm^2/V. This estimate is similar in sign and magnitude to the quadratic effect found in the study mentioned above but as the non-linear deviation is not much greater than our r_{41} error of 1.7%, we cannot assert a value at this point. The small discrepancy from the linear effect also indicates that if there is any morphic effect present in this structure it is very weak. The width of our wells are in the order of a few tens of lattice constants. If there is a morphic effect one would expect it to be more pronounced in narrower wells.

We intend to examine the discrepancy further by studying the effect at wavelengths to the band edge. In this way we expect to separate the morphic from the quadratic effect, as a possible morphic effect would be less dependent on wavelength than the quadratic electro-optic effect. The latter is directly related to the fundamental band gap and should therefore get larger as we approach the band-edge.

The built-in birefringence $\Delta\phi_0$ depends on the optical dielectric profile and the stress birefringence. The stress birefringence contribution is due to the difference of the thermal expansion coefficients of GaAs and of AlGaAs. $\alpha(\mathrm{GaAs}) = 6.86 \times 10^{-6}\ (°\mathrm{C})^{-1}$ [12] and $\alpha(\mathrm{AlAs}) = 5.2 \times 10^{-6}\ (°\mathrm{C})^{-1}$ [13]. We assume this parameter values linearly with Al content.

In the model [14] used to estimate the stress contribution, it is assumed that the sum of the layer thicknesses is small compared to the extension of the sample and that the radius of curvature is very large compared to the sample thickness. It is also assumed that no external forces and no body forces are applied and that the stresses are caused only by the difference in thermal expansion of the layers. We also neglect edge effects and replace the MQW layer by a homogeneous $Al_{0.14}Ga_{0.86}As$ layer. An average growth temperature of 640°C was used. The calculated value for $\Delta\phi_0$ without the stress term is $\Delta\phi_0 = 1982$ nm/mm. The value with the stress term included is $\Delta\phi_0 = 1671$ nm/mm.

The extrapolated straight curves for the two propagation directions intersect at 1.8 V which is close to the diffusion potential $V_0 \approx 1.4$ V at which $E_j = 0$. The extrapolated experimental value of this phase difference between the TE and TM modes amounts to $\Delta\phi_0 = 1790$ nm/mm. The small difference between the calculated values and our experimental value of $\Delta\phi_0$ gives confidence in our measurement procedure and final results. It should be noted that as the linear extrapolation of the overlap factor is not valid for applied bias larger than $V_a = -2$ V, correction of the experimental fit for a varying Γ would give a more accurate diffusion potential but not change the value of $\Delta\phi_0$.

In summary, the MQW structure sandwiched between $Al_xGa_{1-x}As$ layers forms excellent optical waveguides permitting the determination of the LEO coefficient. The results at $\lambda = 1.1523\ \mu$m show that the dominant phase modulation observed is due to the LEO effect and close to the value of pure GaAs. Morphic and higher order electro-optic effects are weak and can possibly be separated by studying the dispersion of the phase modulation.

We would like to thank W. Schlapp for assistance in the crystal growth. This work was partially funded by the Swiss National Science Foundation.

REFERENCES

[1] W. T. Tsang, Appl. Phys. Lett. *39*, 786 (1981).
[2] T. H. Wood, C. A. Burrus, D. A. B. Miller, D. S. Chemla, T. C. Damen, A. C. Gossard and W. Wiegmann, Appl. Phys. Lett *44*, 16 (1984).
[3] R. Dingle in *Festkoerperprobleme* (*Advances in Solid State Physics*), edited by H. J. Queisser (Pergamon, Braunschweig, 1975), Vol. XV, p. 21.
[4] D. S. Chemla, Helvetica Physica Acta *56*, 607 (1983).
[5] M. Born and E. Wolf, *Principles of Optics*, 3rd edition (Pergamon Press, Oxford 1965).
[6] J. F. Nye, *Physical Properties of Crystals* (Clarendon Press, Oxford 1957).
[7] D. T. F. Marple, J. Appl. Phys. *35*, 1241 (1964).
[8] D. D. Sell, H. C. Casey, Jr. and K. W. Wecht, J. Appl. Phys. *45*, 2650 (1974).
[9] H. C. Casey, Jr. and M. B. Panish, *Heterostructure Lasers, Part A: Fundamental Principles*, (Acad. Press, New York 1978).
[10] I. P. Kaminow and E. H. Turner, *Handbook of Lasers* (The Chemical Rubber Co, Cleveland, Ohio 1971), p. 447.

[11] H. G. BACH, J. KRAUSER, H. P. NOLTING, R. A. LOGAN and F. K. REINHART, Appl. Phys. Lett. *42*, 692 (1983).
[12] E. D. PIERRON, D. L. PARKER and J. B. MCNEELY, J. Appl. Phys. *38*, 4665 (1967).
[13] M. ETTENBERG and R. J. PAFF, J. Appl. Phys. *41*, 3526 (1976).
[14] F. K. REINHART and R. A. LOGAN, J. Appl. Phys. *44*, 3171 (1973).